The evolution of autonomy from two cooperative specialists in the fluctuating environments

Xiaoli Chen[1, 2, †], Miaoxiao Wang[3, 4, †], Laipeng Luo[1], Xiaonan Liu[1], Liyun An[5], Yong Nie[1#] and Xiao-Lei Wu[1, 2, 6#]

[1] College of Engineering, Peking University, Beijing 100871, China

[2] Institute of Ocean Research, Peking University, Beijing 100871, China

[3] Department of Environmental Systems Science, ETH Zürich, Zürich, Switzerland

[4] Department of Environmental Microbiology, Eawag, Dübendorf, Switzerland

[5] College of Architecture and Environment, Sichuan University, Chengdu, 610000, China

[6] Institute of Ecology, Peking University, Beijing 100871, China

[†]These authors contributed equally

[#]Corresponding author: Research Scientist, College of Engineering, Peking University.

Tel: +86 10-62759047; Fax: +86 10-62759047; E-mail: nieyong@pku.edu.cn

[#]Corresponding author: Professor, College of Engineering, Peking University.

Tel: +86 10-62759047; Fax: +86 10-62759047; E-mail: xiaolei_wu@pku.edu.cn

Abstract

From microbes to humans, all organisms perform numerous tasks for their survival, including food acquisition, migration, and reproduction. A complex biological task can be performed by either an autonomous organism or cooperation among several specialized organisms. However, it remains unclear how Autonomy and cooperation evolutionarily switch. For example, when an autonomous organism is selectively favored, can the group of cooperative specialists evolve into the autonomous organism? Here, we address this question by experimentally evolving a mutualistic microbial consortium composed of two specialists that cooperatively degrade naphthalene. We observed that autonomous genotypes capable of performing the entire naphthalene degradation pathway evolved from two cooperative specialists and came to dominate the microbial community. This evolutionary transition was driven by the horizontal gene transfer between the two specialists. However, this evolution was exclusively observed occurs in the fluctuating environment supplied with either naphthalene or pyruvate, where mutualism and competition between the two specialists alternated. The naphthalene-supplied environment exerts selective pressure that favors the expansion of autonomous genotypes but was associated with low cell density and coexistence levels. In contrast, the pyruvate-supplying environment promoted the coexistence and cell density of the cooperative specialists, thereby increasing the likelihood of horizontal gene transfer. Using a mathematical model, we quantitatively showed that environmental fluctuations facilitate the evolution of autonomy through HGT when the relative growth rate and carrying capacity of the cooperative specialists allow enhanced coexistence and higher cell density in the competitive environment. Together, our results demonstrate that mutualistic cooperation can evolve combinedly into autonomous organisms through direct genetic exchange under specific conditions, including the alternation of mutualism and competition in fluctuating environments that frequently proceed in nature.

Introduction

Bio-organisms perform diverse biological tasks in response to numerous pressures for survival, from hunting for food to reproducing and raising offspring. Biological tasks can be autonomously finished by one organism itself, or through the cooperation of social organisms working together for common or mutual benefits[1,2]. The trade-off between Autonomy and cooperation can be found at all levels of biological organization. It is even commonly observed that a specific type of task is achieved by either of the two strategies in different organisms. For example, many animal predators, such as tigers (*Panthera tigris*)[3], cheetahs (*Acinonyx jubatus*)[4], and golden eagles (*Aquila chrysaetos*)[5], always hunt alone. In contrast, predators like lions (*Panthera leo*)[6], hyenas (*Hyaenidae*)[7], killer whales (*Orcinus orca*)[8], and Harris' Hawks (*Parabuteo unicinctus*)[9], prefer to form parties composed of multiple individuals to hunt via cooperation. Bacteria operate the nitrification pathway to acquire available energy, which is often conducted by mutualistic cooperation (refers specifically to the cooperation between different populations): ammonia-oxidizing bacteria convert ammonia to nitrite and nitrite-oxidizing bacteria convert nitrite to nitrate[10]. However, *Nitrospira* bacteria are identified to achieve complete nitrification within a single cell[11-13]. Similarly, anaerobic degradation of long-chain alkanes can be either performed via mutualistic cooperation between alkane-oxidizing bacteria and methanogenic archaea (known as syntrophy)[14] or by an autonomous archaeon, namely *Candidatus* Methanoliparum[15].

Organisms evolve to perform either the autonomy or cooperation selected by the environments they reside in to improve the success of the given task[16,17]. For instance, bacteria performing autonomous nitrification are favored in biofilms because biofilms restrain the spatial intermixing of the multiple cooperative specialists, and diffusion barriers in biofilms limit the exchange of metabolites among different individuals, which is necessary for the metabolic cooperation[13,18]. Many studies also propose principles to clarify the general criterion when

68 cooperation or Autonomy is favored[19,20]. However, we lack the knowledge to address whether
69 Autonomy and cooperation can evolutionarily switch in nature[21]. For example, when the
70 cooperation fosters higher productivity, can an autonomous organism divergently evolve to be
71 different cooperative genotypes? Reversely, when an autonomous organism is selectively
72 favored, can the group of cooperative specialists evolve into the autonomous organism? Such
73 evolutionary transitions are essential for the adaptation of bio-organisms to their changing
74 habitats. Several hypotheses have been proposed to address the evolution of cooperation from
75 an autonomous ancestor. For example, the Black Queen hypothesis predicts that this process is
76 originally driven by the leakiness of public goods[22,23]. This prediction explains the evolution
77 of cooperation in several cases[24-27], and has been tested by a few conceptual models[17,22,28], as
78 well as in the experimental evolution of *Pseudomonas aeruginosa*[29] and engineered
79 *Saccharomyces Cerevisiae*[30].
80 In comparison, our understanding of the co-evolution of different cooperative specialists
81 toward Autonomy is more lacking, for which two possible ways are hypothesized[31]. First, one
82 of the cooperative specialists coopts its lacking function by evolving itself. One study observed
83 this pathway in the experimental evolution of pellicle biofilms of *Bacillus subtilis*, in which
84 one of the ancestral cooperative genotypes evolve to form biofilm autonomously independent
85 of its partner[32]. Second, one the cooperative specialist obtains the lacking function from its
86 cooperative partner. In specific to cooperation among different genotypes, this pathway is can
87 be mediated via horizontal gene transfer (HGT)[33,34] among different cooperative specialists.
88 Several studies suggest that mobile genetic elements (plasmids, bacteriophages, transposons,
89 etc.) transmitted via HGT often carry multiple traits that can complement the functional deficits
90 of the auxotrophic organisms[35-37]. One recent study assesses the effect of HGT on bacterial
91 metabolic networks using 835 genomes[21]. They found that HGT can add new catabolic routes
92 to bacterial metabolic networks, potentially augmenting the function of the bacteria. These

genomic analyses strengthen the prediction that Autonomy can evolve from the mutualistic cooperation through genetic transfer between different organisms. However, experimental evidence is still lacking.

Another crucial aspect to consider is the impact of environmental fluctuations that frequently occur in natural habitats[38]. These fluctuations have been shown to influence evolution, particularly the co-evolution of different genotypes[39]. First, the fitness of a novel mutant is varied among different environments. In a constant environment, the fate of mutation is mostly decided by its fitness in the given environment. In comparison, whether a mutation can be fixed in a fluctuating environment is determined by both its average fitness across environments and the frequency of environmental fluctuations[40]. Second, environmental fluctuations can also influence the coexistence of different genotypes because relative fitness and ecological interactions between different genotypes can be varied in different environments[38]. Several studies suggest that environmental fluctuations promote the coexistence of different genotypes[41-43]. In such cases, environmental fluctuations may benefit the coevolution of different genotypes, for example, by improving the HGT rate among these genotypes. In the case of the evolution of autonomy from cooperation, it requires: 1) the evolved autonomy possesses higher overall fitness (adaption); 2) the cooperative specialists can co-exist to enable HGT. Environmental fluctuations can influence both these two aspects.

Here, we experimentally tested whether a mutually cooperative consortium can evolve into an autonomous organism and how environmental fluctuations influence the evolution. We performed this study by evolving a mutualistic consortium composed of two bacterial specialists that cooperatively degrade naphthalene in constant and fluctuating environments. Based on our experimental findings, we built a mathematical model to search the key factors that determine whether autonomy can evolve from a mutualistic cooperation.

Results

The design of the synthetic consortium and the experimental evolution

The synthetic mutualistic consortium used for the experimental evolution is modified from our previous study[44]. In this consortium, the first strain (referred to as the Degrader thereafter) degrades naphthalene to salicylate, which is further decomposed into small molecules such as pyruvate by the second strain. The Degrader is able to grow alone using naphthalene as the sole carbon source while the second strain cannot (Figure 1A-B; Figure S1). Notably, salicylate is found to be toxic to both strains[45,46] (Figure S2), thus indicating that the second strain also contributes to the detoxification process (hence we refer to the second strain as the Detoxifier thereafter; Figure 1B), as confirmed by our coculture experiment (Figure S2). Similar forms of cooperative degradation of organic compounds have been frequently observed[47-55]. Our experiment also suggested that the two strains showed facultative mutualism upon co-culture (Figure S1). We engineered the two strains in this consortium from an ancestral *Pseudomonas stutzeri* strain, which can completely degrade naphthalene into small molecules (referred to as Autonomy thereafter; Figure 1C). When culturing the Autonomy or the mutualistic consortium using naphthalene as the sole carbon source, the Autonomy exhibits a higher growth rate and biomass yield than those of the consortium (Figure 1A). Moreover, we inserted specific barcode tags and fluorescent genes into the chromosomes of these strains to distinguish them during the coculture and evolution experiments (Methods; Table S1).

We performed the experimental evolution by consistently passaging the cultures of the consortium in three different environments distinguished by different carbon source supplements (Figure 1D): (1) naphthalene was supplied in every passaging cycle as the sole carbon source, so two strains within the consortium engaged in mutualistic cooperation throughout the evolution (referred to as the mutualism condition thereafter); (2) pyruvate, which can be used by both strains for growth (Figure 1B), was supplied in every passaging

142 cycle so both strains compete for the sole carbon source (referred to as the competition
143 condition thereafter); (3) To mimic environmental fluctuations, naphthalene or pyruvate was
144 alternately supplied in the passaging cycles so the two strains alternately engaged in mutualism
145 or competition in different cycles (referred to as the fluctuating condition thereafter). To
146 capture the effects of the potential stochastic events, we conducted 12 experimental replicates
147 for each condition (i.e., 36 evolutionary lineages in total). With these set-ups, we explored
148 whether autonomous genotypes could evolve from the mutualistic consortium after the
149 experimental evolution under these conditions.

150 **Distinct evolutionary strategies under different environmental conditions**

151 To investigate the evolutionary fates of our mutualistic consortium under different conditions,
152 we tracked the dynamics of the two strains in all the evolutionary lineages and measured the
153 phenotype changes of the evolved populations, including their growth and tolerance to
154 salicylate toxicity.

155 *The Degrader dominated the community when our mutualistic consortium evolved under the*
156 *mutualism condition.*

157 In the mutualism condition, we observed that the Degrader rapidly dominated all the lineages
158 Figure 2A). After 280 generations, we did not detect specific genes in the Detoxifier, *nahG* and
159 *nahTH*, in all lineages in the mutualism condition, suggesting the collapse of the cooperation
160 between the Degrader and Detoxifier (Figure S3). When we cultured the evolved consortia
161 using naphthalene as the sole carbon source, we found that these consortia exhibited
162 significantly higher growth rates than the ancestral mutualistic consortium (T-Test, $p < 0.05$)
163 but their maximum cell densities (OD_{max}) did not increase after evolution (T-Test, $p > 0.05$;
164 Figure 2B; Figure S4A). Next, we spread the cultures of these lineages on agar plates and
165 picked four single colonies from each lineage. We sequenced their barcode tags, which
166 confirmed these isolated strains all evolved from the ancestral Degrader strains (Table S1).

When cultured in the minimal medium supplemented with naphthalene, we observed three distinct phenotypes in these isolated strains as compared to the ancestral Degrader: (1) the first group of strains grew faster than the ancestral Degrader but their tolerance to salicylate toxicity did not change significantly (as surrounded by a blue oval in Figure S4B); (2) the second group did not increase in growth rate but evolved to be higher tolerant to salicylate toxicity (as surrounded by an orange oval in Figure S4B); (3) the third group evolved to possess both higher growth rates and higher tolerance (as surrounded by a red oval in Figure S4B). Interestingly, we found that the first and second groups coexisted in lineage 6 after evolution (Figure S4B), suggesting that a novel form of niche differentiation between the two populations evolved after 280 generations in the mutualism condition. In addition, the third phenotype evolved and dominated in lineages 1 and 10 (Figure S4B), indicating that the ancestral Degrader strain was able to evolve and compensate for its deficiency (i.e., salicylate tolerance) by evolving itself. This observation parallels the findings from another study where the collapse of mutualistic cooperation was observed. In that study, a *Bacillus subtilis* strain deficient in biofilm formation was able to regain complete functionality and form a biofilm through self-evolution[56]. Similarly, in both our experiment and this previous study, one of ancestral genotypes compensates for its lacking function by evolving a new function on its own, enabling them to thrive more effectively in their respective habitats. Together, these results demonstrate that the mutualistic cooperation between the Degrader and Detoxifier strains in the ancestral consortium collapses under the mutualism condition. Furthermore, we observed the evolution of either a novel form of niche differentiation or a single population with improved survival. However, we did not observe the evolution of an autonomous genotype that can perform the entire pathway of naphthalene degradation.

190 *Diverse community structure emerged when our DOL consortium evolved in the competition*
191 *condition.*
192 When passaging our DOL consortium under the competition condition, we observed that the
193 Degrader decreased in frequency during the early stages of the passage in all lineages, and this
194 decrease persisted for approximately 100 generations in eleven of twelve lineages (Figure S5A).
195 This decrease was due to the higher fitness of the Detoxifier in pyruvate-supplied enviroments
196 than that of the Degrader (Figure S5B-D). However, the frequencies of the Degrader of these
197 lineages gradually exhibited significant variations after 100 generations, with the relative
198 frequency of the Degrader strain ranging from 0.05 to 0.96 at the 268 generation. Specifically,
199 the relative frequency of the Degrader strain exceeded the initial frequency of the inocula in
200 six of twelve lineages (Figure S5A). These results suggest that although the ancestral
201 Dextoxifier showed higher fitness than ancestral Degrader, potentially hindering their co-
202 existence in the competition condition, the Degrader may evolve to possess varied fitness,
203 leading to diverse community structures.
204 *The evolution of autonomy from the cooperative specialists under the fluctuating environment.*
205 When evolving our mutualistic consortium in the fluctuating condition, we found that the
206 relative frequency of the Degrader shows oscillating dynamics in most of the lineages (Figure
207 2C). Specifically, the Degrader shows higher frequencies in the naphthalene-supplied cycles,
208 but its frequency decreases when the cultures were passaged to the pyruvate-supplied cycles
209 (Figure 2C). These results indicated that the introduction of pyruvate-supplying cycles, where
210 both strains engaged in resource competition, served to rescue the collapse of their coexistence
211 occurring in the mutualism condition. Interestingly, when we cultured the evolved consortia
212 using naphthalene, we found that consortia from five of the twelve lineages exhibited higher
213 maximum biomass yield than the ancestral mutualistic consortium, namely lineage No.1, No.4,
214 No.6, No.7 and No.11 (Figure 2B; Figure S6A). We next spread the cultures of these five

evolved consortia on agar plates and picked four single colonies from each lineage. We found all these isolates could grow alone using naphthalene. 14 out of 20 isolates showed similar or higher OD_{max} as the Autonomy strain and 20 out of 20 isolates showed similar or higher growth rates as the Autonomy strain (Figure 3A, Student's T-test, $p < 0.05$; Figure S6B).

To explore the genetic underpinnings behind the improved growth of these isolated strains using naphthalene, we conducted whole-genome sequencing on all isolates. We first checked the genomic locations encoding the two operons of naphthalene degradation genes. Surprisingly, we found that all isolates evolved to reobtain a copy of the previously deleted naphthalene degradation genes (Figure 3B-C), potentially via HGT from its cooperative partner. Notably, these regained genes locate exactly at the same genomic locus as that of our ancestral Autonomy strain (Figure 3B-C), suggesting that the genes are regained via homologous recombination[57,58], one widespread mechanism benefiting HGT among different bacteria[59]. To eliminate the possibility that these observed Autonomy strains are derived from the contamination of the lab-stored Autonomy strain, we checked the sequence of the barcode tags. We found that the strains from three of the five lineages possess the same barcode tag as the ancestral Degrader strain, while the strains from two of the five lineages possess the same barcode as the ancestral Detoxifier strain (Table S2). This result indicates that the observed Autonomy strains evolved from either the Degrader or the Detoxifier strain during the evolution. Together, these results indicate that the ancestral cooperative specialists in our mutualistic consortium can evolve combinedly into Autonomy, potentially driven by HGT. Nevertheless, this evolution only occurred in the fluctuating condition where naphthalene and pyruvate were alternately supplied.

The fluctuating environment creates important conditions for the evolution of autonomy.

Why is fluctuating environment mandatory for the evolution of autonomy in our experiment? In other words, why both mutualism and competition cycles are required? We offer three points

240 to explain the results. First, we observed that the evolved Autonomy exhibited faster growth
241 and higher maximum biomass yield compared to the mutualistic consortium when grown on
242 naphthalene as the carbon source (Figure 1A). However, this growth advantage was not
243 observed in the medium supplemented with pyruvate (Figure S5). Furthermore, we observed
244 that the evolved genotypes under competition conditions, where pyruvate served as the sole
245 carbon source in all cycles, exhibited a lower capability for naphthalene degradation (Figure
246 S7A-B) and the autonomous genotype did not evolve in this condition (Figure S7C). This result
247 indicates that the competition cycles alone did not favor the evolution of the autonomous
248 genotype. Together, these findings suggest that the naphthalene-supplied cycles are crucial to
249 exert selective pressure in favor of Autonomy over mutualistic cooperation and are therefore
250 also necessary for the evolution of autonomy in our experiments.
251 Second, we observed that the Degrader and Detoxifier exhibited a low level of coexistence in
252 cycles supplemented with naphthalene, with the Degrader dominating. However, in cycles
253 supplemented with pyruvate, we observed a significant improvement in their coexistence
254 (Figure 2C). This increase in coexistence is attributed to the higher fitness of the Detoxifier in
255 pyruvate-supplied cycles than the Degrader, as shown in Figure S6, resulting in an increase in
256 its frequency and facilitating its coexistence with the Degrader. Although we observed that the
257 Degrader may evolve to possess higher fitness after the evolution under the competition
258 conditions, our results suggested that the Autonomy evolved at an earlier stage of the evolution,
259 spanning 33 to 114 generations (Figure 3D), preceding the stage where the Degrader evolved
260 to higher fitness. The increased coexistence is expected to benefit the evolution of Autonomy
261 via HGT because the coexistence of the donor and recipient is the prerequisite for HGT[33]. To
262 further examine the importance of co-existence, we performed evolution experiments on
263 twelve novel lineages under the mutualism condition. Although the Degrader rapidly
264 dominated the community in these lineages thus Degrader and Detoxifier showed low co-

265 existence level, we manually re-added new Detoxifier cells to the cultures to increase the co-
266 existence. We found that Autonomy evolved in three of the twelve lineages (Figure 4). This
267 result confirmed that the better coexistence of the Degrader and the Detoxifier in the
268 competition cycles plays a key role in driving the evolution of Autonomy via HGT.
269 Third, the mutualistic consortium accumulates higher cell density in the pyruvate-supplied
270 cycles (OD_{600}: ~1.0) than that in the naphthalene-supplied cycles (OD_{600}: ~0.4; Figure S8).
271 Previous studies reported that higher cell density increases HGT rates[60], potentially by
272 increasing the chance of cell-cell or cell-mobile genetic elements contact[61,62]. Thus, the
273 increase in cell density in the pyruvate-supplied cycles may increase the HGT rates between
274 the Degrader and the Detoxifier, and further benefits the evolution of Autonomy.

275 **Mathematical modeling of the evolution of autonomy**

276 *Quantitative explanations for the evolution of autonomy from the mutualistic consortium under*
277 *fluctuating conditions.*

278 To gain quantitative insights into why the fluctuating condition led to the evolution of
279 autonomy in our experiments, we developed a mathematical model grounded on three key
280 assumptions derived from our experimental observations. First, we considered two growth
281 environments: (1) An environment that allows for the facultatively mutualistic cooperation
282 between the Degrader and the Detoxifier (referred to as environment (Mutual.) thereafter),
283 where the Degrader degrades a substrate into a toxic intermediate, and the Detoxifier further
284 metabolizes this intermediate for detoxification (Figure S9A). (2) An environment where both
285 strains compete for limited resources (referred to as environment (Comp.) thereafter). Second,
286 the Autonomy can evolve from any of the Degrader and the Detoxifier via HGT. We assumed
287 that the HGT probability positively correlates to the cell density and the co-existence level of
288 the Degrader and Detoxifier[63,64] (Methods). Third, we assumed that the evolved autonomous
289 genotype possesses a growth advantage (in terms of both growth rate and biomass yield) in the

290 environment (Mutual.) but not in the environment (Comp.). Based on these assumptions, we
291 built an ODE system (Methods: Eqn. [2] to [10]) to mimic two important conditions in our
292 experiments: (1) the mutualism condition where the initial consortium is passaged continually
293 in the environment (Mutual.); (2) the fluctuating condition in which the consortium grows
294 alternately in the environment (Mutual.) and the environment (Comp.).
295 To reproduce the basic findings of our experiments, we performed simulations initialized with
296 the parameters obtained from our experimental system (Table S3: default values). Out of 100
297 replicated simulations of the fluctuating condition, we found that Autonomy evolved in 59
298 replicates within 50 dilution cycles (Figure 5A-C); in comparison, Autonomy only evolved in
299 16 of 100 replicates in the mutualism condition (Figure 5D-E). This result agrees with our
300 experimental findings, suggesting that environmental fluctuations facilitate the evolution of
301 autonomy within the conditions of our experiments.
302 Our experiments suggested two important hypotheses regarding how the environment (Comp.)
303 in the fluctuating conditions select for the evolution of autonomy via HGT: (1) the higher
304 fitness of the Detoxifier in the environment (Comp.) increases the co-existence of both strains
305 so benefit the HGT; (2) the higher cell density in the environment (Comp.) facilitates the
306 evolution of autonomy. To quantitatively examine the first hypothesis, we set the carrying
307 capacity of the two environments to be the same (so exclude the effects of the difference in cell
308 density). We performed simulations parameterized with varied relative growth rates between
309 the Degrader and Detoxifier. The result showed that the evolution of autonomy was favored
310 under the fluctuating condition when the growth rate of the Detoxifier fell within a specific
311 range: higher than that of the Degrader but lower than a threshold value (Figure 5F). Our
312 analysis shows that this range closely corresponded to the range in which the coexistence level
313 of the two strains is higher under the fluctuating condition compared to the mutualism condition
314 (Figure S9B). These results provide compelling evidence that a certain degree of higher fitness

315 of the Detoxifier in the environment (Comp.) positively impacts HGT by promoting co-
316 existence, supporting our first hypothesis. To test our second hypothesis, we performed
317 additional simulations by setting the carrying capacity of the environment (Comp.) to be twice
318 that of the environment (Mutual.), in line with the scenario of our experiment. We found that
319 higher cell density in the environment (Comp.) expanded the parameter range in which the
320 fluctuating condition promotes the evolution of autonomy (Figure 5F-G). Furthermore, we
321 observed that this range can be predicted by combining the effects of cell density and
322 coexistence level (Figure S9B-C). Together, these simulations demonstrate that environmental
323 fluctuations play a crucial role in introducing variations in relative fitness and cell density,
324 thereby facilitating the evolution of autonomy through HGT within specific conditions.

325 *The impact of fluctuating environments on the evolution of autonomy is dependent on specific*
326 *pathways conditions*

327 To test the prevalence of our experimental finding, we performed simulations using 17501
328 randomly-sampled parameter sets, each of which defined a specific condition of pathway
329 kinetics and strain growth (Methods; Table S3). For a given set, we modeled both the
330 mutualism condition and the fluctuating condition with 20 replicates for each, which allowed
331 us to calculate the frequency of the Autonomy evolution in both conditions (defined as P_{mut}
332 and P_{fluc}). As shown in Figure 6A, we observed that the Autonomy evolved in at least one of
333 the two conditions in the simulations conducted with 13905 parameter sets, accounting for 79.4%
334 of all simulated sets. Notably, 2269 of these sets (~12.9%) resulted in a scenario closely
335 resembling our experimental observations, in which the autonomous genotype exclusively
336 evolved in the fluctuating condition. In comparison, a smaller number of sets (1003, ~5.7 %)
337 enabled the simulations where the autonomous genotype only evolved in the mutualism
338 condition. Moreover, among the simulations where the autonomous genotype evolved in both
339 conditions (10633 of 17501 sets, ~60.8%), we observed a significantly higher frequency of the

340 mutualism consortium evolving into an autonomous genotype in the fluctuating condition
341 compared to the mutualism condition (Figure 6B; $p < 0.001$). Collectively, these results
342 indicate that the influence of fluctuating environments on the evolution of autonomy is
343 dependent on the specific conditions of the pathways involved. Nevertheless, fluctuating
344 environments generally enhance the probability of Autonomy evolution.

345 *Key factors determining the evolution of Autonomy from mutualistic cooperation.*

346 To investigate the key factors defining whether Autonomy can evolve in the mutualism
347 condition or the fluctuating condition, we compared the distributions of parameter values that
348 enabled the evolution of Autonomy in simulations to those that did not. We identified five of
349 14 parameters that significantly affect whether Autonomy can evolve from the mutualism
350 condition (Figure S10; Kolmogorov-Smirnov Test: $p < 0.01$). This deduction is further
351 supported by Pearson correlation analysis between the parameter set and the frequency of the
352 Autonomy evolution in the corresponding simulations (Figure 6C; correlation coefficients over
353 0.1). Using the identical methods, we identified eight of 13 parameters that significantly affect
354 whether Autonomy can evolve from the fluctuating condition (Figure S11; Kolmogorov-
355 Smirnov Test: $p < 0.01$; Figure 6D). Furthermore, our analysis suggested that ρ_M (maximum
356 carrying capacity in the environment (Mutual.)) positively affected cell density and coexistence
357 levels in the mutualism condition (quantified by BCI_M, see Equation [11]), thereby facilitating
358 the evolution of Autonomy (Figure 6C). Similarly, ρ_M, ρ_C (maximum capacity in the
359 environment (Comp.)), and $\sigma_{c,Detox}$ (Relative growth rate of Autonomy to that of Degrader in
360 the environment (Comp.)) positively impacted cell density and coexistence levels under the
361 fluctuating condition (quantified by BCI_{M+C}), consequently benefiting the evolution of
362 Autonomy (Figure 6D). We also found that $\mu_{m,Degra}$ (Growth rate of Degrader in the
363 environment (Mutual.)) and $\mu_{c,Degra}$ (Growth rate of Degrader the environment (Comp.)),
364 respectively affected the evolution by modifying the duration of each cycle (Figure 6C-D).

365 Higher growth rates shorten the cycle duration (because we passage the consortium once they
366 reach the stationary phase) so reduced the probability of HGT.
367 Finally, we turned to explore the parameters defining when the fluctuating condition benefits
368 the evolution of Autonomy compared to the constant mutualism condition. We hypothesized
369 that environmental fluctuations would be beneficial when the mutualistic consortium exhibits
370 a higher cell density and better coexistence of the two strains in the environment (Comp.)
371 compared to the environment (Mutual.). To examine this hypothesis, we conducted a
372 correlation analysis between a Relative Biomass-Coexistence Indice ($BCI_{C/M}$; Methods) to a
373 Fluctuation-Benefiting Index (FBI; evaluating the degree that fluctuating conditions benefit the
374 evolution of autonomy; Methods). Our analysis revealed a significant positive relationship
375 between $BCI_{C/M}$ and FBI, supporting our hypothesis ($p < 0.001$; R^2=0.41). We also found a
376 positive correlation between the relative duration of growing in the environment (Comp.)
377 versus the environment (Mutual.) (Refer to as $T_{C/M}$ thereafter) and FBI ($p < 0.001$; R^2=0.35),
378 suggesting that longer duration in the environment (Comp.) also benefit the evolution of
379 autonomy. Through Pearson correlation analysis, we identified key model parameters that
380 largely affect $BCI_{C/M}$ and $T_{C/M}$ (Figure 6E): (1) ρ_m negatively influences the values of $BCI_{C/M}$
381 while ρ_c and $\sigma_{c,Detox}$ (Relative growth rate of Detoxifier to that of Degrader in the environment
382 (Comp.)) affects $BCI_{C/D}$ positively. (2) $T_{C/M}$ is positively impacted by $\mu_{m,Degra}$ while negatively
383 altered by $\mu_{c,Degra}$. In summary, our findings suggest that the evolution of Autonomy in the
384 mutualistic consortium is promoted by a fluctuating condition when the consortium exhibits
385 increased cell density, enhanced co-existence, and prolonged growth in the environment
386 (Comp.). These factors are determined by the relative growth rate and capacity in the two
387 environments.
388

Discussion

Here, we provided experimental evidence that a consortium engaged in mutualistic cooperation can evolve combinedly into an autonomous genotype via horizontal gene transfer (HGT). We show experimentally that environmental fluctuations are important to drive such evolution and mathematically identify the key parameters that determine when fluctuating environments are beneficial.

Within human economies, Adam Smith proposed that cooperation will emerge from Autonomy in order to achieve higher productivity[65]. This concept has been applied to understand the evolution of natural biological systems and any studies have discussed when and how cooperation can evolve from an autonomous ancestor[2,19,20,66-68]. However, Autonomy is favored in many specific environments over cooperation in nature. Therefore, it is also crucial to understand how Autonomy can evolve from cooperation if it shows better adaption and higher productivity. Such evolution is particularly critical in scenarios where cooperation initially evolved in an environment that favored cooperation, but later shifted to favor Autonomy. Genetic exchange (e.g., HGT) among natural partners may help a cooperative specialist regain deficient function, which could mediate the collapse of cooperation and the evolution of Autonomy. Here in this study, we provide the first experimental evidence for this hypothesis. In addition, a recent review put forth an intriguing prediction, suggesting that less dependent mutualisms, such as facultative mutualisms, are more likely to transition back to autonomy compared to highly dependent mutualisms, such as obligate mutualisms[69]. Given that the two cooperative specialists in our consortium display facultative mutualism, our results provide experimental evidence supporting this prediction.

Our study highlights that environmental fluctuations affect such evolution. Since natural populations often experience fluctuations in nutrient types in their environment[38], we would expect that this effect is prevalent in nature. The underly mechanism of this finding is that

414 environmental fluctuations impact both the selection pressure on the autonomous genotype and
415 conditions for HGT (i.e., high cell density and the coexistence of both genotypes). We would
416 specifically point out the importance of coexistence to drive these kinds of co-evolution of
417 different genotypes. In our case, HGT generally requires different genotypes co-exist to enable
418 the sharing of their genetic elements[21,33,62]. In another case, two mutualistic *E.coli* partners
419 evolve to form multicellular spatial clusters that benefit their cooperation, and this evolution
420 requires the coexistence of both partners[70]. In addition, *Pseudomonas aeruginosa* evolved to
421 increase resistance towards beta-lactam antibiotics when coexisting with *Staphylococcus*
422 *aureus*[71]. Therefore, co-existence allows genetic exchange and group-level selection that drives
423 evolutionary innovations.
424 The idea of increasing species co-existence has implications for the artificial selection of high-
425 function microbiomes[72-74], in which we should ensure the co-existence of different organisms
426 to enable the evolution towards higher function. Our work offers a potential approach in which
427 we can select a microbiome in fluctuating nutrient conditions. However, fluctuating
428 environments are not always useful to maintain co-existence. For example, one recent study
429 reported that the rapid evolution of one partner in a fluctuating environment collapsed the long-
430 term co-existence of two species engaged in positive pairwise interactions[75]. For a quantitative
431 understanding, our mathematical model can be used to predict whether this method is efficient
432 in allusion to a specific system. Another method suggested by our experiments is to re-add the
433 seeding species, which mimics the immigration events in nature[76]. As re-add the Detoxifier
434 cells also enables the evolution of Autonomy, re-supplying the key seeding species to the
435 selection systems may also increase their function.
436 We also observed randomness in our experiments: only five of the twelve lineages evolved to
437 Autonomy. We speculated several stochastic factors that lead to this outcome. First, the
438 occurrence of HGT events is random, which requires the occasional cell-cell or cell-mobile

genetic elements contact[61,62]. Second, the co-existence of both genotypes and the expansion of an autonomous genotype is also affected by random factors, including the bottleneck effects occurring during the culture dilution at the beginning of each cycle[77,78], as well as phenotypic variations of the seeding cells among different lineages. In summary, the evolution of Autonomy requires that the HGT events occur before the co-existence of two genotypes collapses, and the evolved autonomous genotype can overcome other random factors to successfully fix in the community. Similar phenomena were observed or characterized in other studies. For instance, while *E. coli* usually outcompetes *Saccharomyces cerevisiae* in co-culture, one study shows that a few lineages of *S. cerevisiae* could evolve to coexist by mutating multi-hit genes before they were excluded by *E. coli*[79]. Therefore, the chronological order of evolutionary innovations and the loss of coexistence, determined by stochastic factors, is key to shaping the outcomes of the co-evolution. This finding suggests that more replicates are required for further evolution experiments.

In conclusion, our study addressed the knowledge gap regarding whether Autonomy can evolve from mutualistic cooperation through genetic transfer. Our finding suggests that biological systems can adapt to complex environments by evolutionarily switching their living strategies. We also provide novel insights into manipulating the co-evolution of different species towards artificial systems with high and desired functions.

461 **Methods**

462 **Construction of the strains used in this study**

463 The strains and plasmids used in this study were summarized in Table S4. We used a previously
464 developed experimental microbial system for naphthalene degradation, which is described
465 elsewhere[44]. Briefly, Autonomy can degrade naphthalene to the final products (pyruvate and
466 acetyl-coenzyme A). Degrader contains a deletion in *nahG* (encodes a salicylate hydroxylase)
467 and *nahTH* (encodes a catechol 2, 3-dioxygenase) genes, so can only oxidize naphthalene to
468 salicylate, during which byproduct pyruvate is generated to support its growth. Detoxifier
469 contains a deletion in *nahA* (encoding a naphthalene dioxygenase) and *nahC* (encoding a 1, 2-
470 dihydroxynaphthalene dioxygenase) genes, so can only convert salicylate to the final products.
471 To distinguish ancestral genotypes during evolutionary experiments, ancestral Autonomy,
472 Degrader, and Detoxifier were engineered to carry unique DNA barcodes (Table S1-2). To
473 measure their relative abundance in the consortia, Degrader and Detoxifier were labeled with
474 *mCherry* and *eGFP,* encoding rea and green fluorescent proteins. Therefore, the DNA
475 fragments of the *barcode* and *mCherry* gene, or the *barcode* and *eGFP* gene, were cloned into
476 a vector, pUC18T-mini-Tn7T-Gm[80] (Table S4). The derived vector was delivered to host cells
477 via conjugative four-parental mating. As a result, these fragments were knocked into the
478 chromosomes of these strains at Tn7 attachment (attTn7) sites[81]. *P. stutzeri* exconjugants were
479 selected in solid LB supplemented with nalidixic acid (5 μg/mL) and gentamycin (25 μg/mL).
480 To prevent contamination during the evolution experiment, FRT excision of the gentamycin
481 resistance marker was not performed, and all of the ancestral strains retained gentamycin
482 resistance.

483 To observe the evolution of consortia over a relatively short time, the mutation rates of strains
484 were improved by regulating the expression of the *mutS* gene (Figure S12). The promoter
485 *rhaSR-PrhaBAD* induced by L-rhamnose was inserted in front of the *mutS* gene. During the

evolutionary experiments, L-rhamnose was not added to the medium, and *mutS* was not expressed, leading to a higher spontaneous mutation rate due to the inactivation of the methyl-directed mismatch repair system[82]. After the evolutionary experiments, bacteria grew in the presence of L-rhamnose (0.2% w/v) for DNA extraction and preparation of growth curve measurement experiments. The expression of *mutS* resulted in a lower spontaneous mutation rate. This genetic modification was implemented by allele exchange using the suicide plasmid pK18mobsacB[83,84].

Salicylate tolerance assays

To measure the tolerance ability of ancestral and evolved strains to salicylate, under antibiotic treatments, overnight cultures were diluted and incubated with an initial OD_{600} (optical density at 600 nm) of 0.05 in fresh minimal medium supplemented with 5 g/L pyruvate and 40 C-mM salicylate along with no-antibiotic negative control. Bacterial cultures were grown at 30°C with shaking at 200 rpm. OD_{600} was measured when the bacteria entered stationary phase. The tolerance ability of bacteria to salicylate were determined as the percentage increase or decrease compared to when bacteria were grown in the absence of antibiotics.

Culture condition and the evolution experiments

Bacterial cultures were grown at 30°C on an orbital shaker set to 200 rpm. Pre-cultures were prepared by cultivating a single isolated colony from a lysogeny broth (LB) plate in the rich medium[85] (Yeast extract 10 g/L, beef extract 5 g/L, peptone 10 g/L, ammonium sulfate 5 g/L) until late-exponential phase (~12 h). Pre-cultured cells were centrifuged and washed three times with the minimal medium[86] prior to the start of the experiments. The seed of the synthetic consortium was made by equally mixing the Degrader strain and the Detoxifier strain. Then the cultures were inoculated with an initial OD_{600} of 0.05 and performed in the minimal medium supplemented with pyruvate (0.5% w/v) or naphthalene powder (1% w/v) as the sole carbon source. The cultures were performed in 20-mL scintillation containing 4 mL of the medium.

511 The evolution experiments were performed under three different conditions of carbon source
512 supplement (Figure 1). (1) the mutualism condition. The consortium was propagated through
513 65 growth-dilution cycles in the minimal medium supplemented with naphthalene as the sole
514 carbon source. The consortium was initially transferred every three days for a total of 24
515 transfers, following 41 transfers every two days. The cultures were diluted by a factor of 20
516 into fresh media during each transfer (~4.3 cellular divisions per growth cycle). The
517 experiments lasted for a total of 154 days, corresponding to approximately 280 generations of
518 bacterial growth. (2) the competition condition. The consortium was propagated through 40
519 growth-dilution cycles by daily (24 h) transfers in the minimal medium supplemented with
520 pyruvate. During propagation, cells were diluted by a factor of 100 into fresh media, which
521 corresponded to ~6.7 cellular divisions per growth cycle and ~268 cellular divisions over a
522 growth cycle. (3) The fluctuating condition. The culture was propagated by switching between
523 the minimal medium supplemented with naphthalene and the medium supplemented with
524 pyruvate. The naphthalene-supplied cycles lasted for three days at the first 17 cycles, following
525 two days for the rest eight cycles. The pyruvate-supplemented cycles lasted for one day. The
526 cultures were diluted by a factor of 100 into fresh media during each transfer (~6.7 cellular
527 divisions per growth cycle). In total, 41 transfers were performed (~275 generations).
528 In total, 36 experimental evolution lineages were performed, in which 12 independent lineages
529 were evolved in parallel for each condition. Biomass and relative abundances of the two
530 populations were assessed by measuring OD_{600} and fluorescence intensity via
531 spectrophotometry in a plate reader. During the evolution, glycerol stocks (20% glycerol) were
532 prepared every five or six transfers and stored at -80°C for future assays. In the propagation of
533 the mutualism condition, two out of twelve lineages were excluded from further analysis due
534 to the extinction.

535 At the end of the propagation experiment, the evolved consortia were spread on LB agar plates
536 supplemented with 0.2% (w/v) L-rhamnose monohydrate to isolate evolved clones. To
537 determine whether the Autonomy evolved in the cultures and to measure the relative
538 abundances of different genotypes, the four key genes (*nahA*, *nahC*, *nahG*, and *nahTH*)
539 encoding naphthalene degradation, a subset of which were deleted in Degrader and Detoxifier,
540 were amplified by PCR to detect their presence. If all four genes were detected, the clones were
541 identified as the putative evolved Autonomy; If only *nahA* and *nahC* were detected, the clones
542 were identified as the Degrader; If only *nahG* and *nahTH* were detected, the clones were
543 identified as the Detoxifier. For each lineage, 24 clones were randomly picked and PCR tested
544 for each lineage. Next, four putative Autonomy colonies from each lineage were selected for
545 growth kinetics measurement and whole genomic sequencing. The isolates were individually
546 grown overnight in MF supplemented with 0.5% (w/v) sodium pyruvate and 0.2% (w/v) L-
547 rhamnose monohydrate and stored in glycerol (final concentration 20%) at -80°C until further
548 use.

549 **The evolution experiments of re-introducing the Detoxifier and examination of the**
550 **evolved Autonomy.**

551 An experiments was designed to further test whether the coexistence of the Degrader and
552 Detoxifier is the key determinant for the evolution of Autonomy. After our initial evolution
553 experiments, Autonomy did not evolve in all twelve lineages under the conditions of mutualism.
554 A new experimental evolution of the ancestral consortium was performed, in which the
555 Detoxifier was re-added to the culture before each passage (final OD_{600} = 0.025, approximately
556 2.5×10^7 cells). The cultures were passaged for 5 cycles under the mutualism condition. The
557 same methods as shown in the above section are applied to determine whether the Autonomy
558 evolved in the cultures and to measure the relative abundances of different genotypes after
559 evolution.

560 **Flow cytometry**

561 Flow cytometry was performed with a CytoFLEX S (Beckman, USA) flow cytometer. During
562 the coculture of the ancestral Degrader and Detoxifier, genotypes in the cultures were
563 distinguished according to their respective fluorescent labelling (eGFP or mCherry). eGFP
564 fluorescence was detected using a 488 nm excitation laser combined with a FITC (525/40 nm
565 filter) detector. mCherry fluorescence was measured using a 561 nm laser combined with a
566 ECD (610/20 nm filter) detector. Before the measurements, each sample was diluted to 10^{-4} -
567 10^{-6} cells/mL in saline solution. Samples were processed at a fixed flow rate of 30 µL/min for
568 an acquisition time of 1 min. Flow cytometry results were analyzed using CytExpert software.

569 **Growth kinetics of ancestral and evolved consortia and clones**

570 Aliquots (0.1 – 0.2 mL) of ancestral and evolved glycerol stocks were revived in 4 mL of the
571 minimal medium containing 0.5% sodium pyruvate and 0.2% L-rhamnose monohydrate and
572 incubated at 30°C with shaking at 200 rpm. These overnight cultures were washed three times
573 with MF medium. Then, cells were inoculated with an initial OD_{600} of 0.05 and were grown
574 statically at 30°C. Growth curves were measured by analyzing changes in cell density (OD_{600})
575 at regular time intervals, and fitted by the following logistic function[87]:

576 $$Y = \frac{Y_M \cdot Y_0}{((Y_M - Y_0) \cdot e^{-k \cdot t} + Y_0)} \quad [1]$$

577 where Y_0 is the minimum population biomass; Y_M is the maximum population biomass; and k
578 quantifies the curve's steepness. The following demographic parameters were extracted: the
579 maximum predicted value for OD_{600} (Growth yield; unit, OD_{600}) and the maximum rate of
580 biomass increase (Growth rate; unit, h^{-1}).

581 **PCR genotyping**

582 To identify the genotype of evolved consortia and isolates, the evolved consortia and isolates
583 were subjected to PCR amplification using a mix of primers including four primer pairs (Table
584 S5). Every PCR primer pair was designed to only amplify a product when the genome of the

585 sample carried the specific gene sequence. The amount of PCR products depends on the kinds
586 of genes in the sample. In addition, the four amplification products displayed different size,
587 which can be distinguished into different bands by DNA electrophoresis. The Degrader
588 possessed two genes distinct from the Detoxifier (*nahA* and *nahC*). The Detoxifier possessed
589 two genes (*nahG* and *nahTH*) distinct from the Degrader. The Autonomy possessed these four
590 genes. The genotypes of the sample were identified by detecting the presence or absence of the
591 four genes.

592 **Whole-genome sequencing and data analysis**

593 In total, 136 clones were picked from the evolved populations (four clones per lineage; 12
594 lineages for the competition condition and the fluctuating condition, and 10 lineages for the
595 mutualism condition). These clones were grown to saturation in RB media supplemented with
596 0.2% L-rhamnose and 25 μg/mL gentamicin. 1 mL of overnight culture was used to extract
597 DNA. Sequencing library preparation was done by using the DNA library preparation kit
598 (Illumina). DNA sequencing was performed on Illumina Novaseq 6000 with 150 bp paired-
599 end. As the control, two clones from the ancestral Degrader population and two clones from
600 the ancestral Detoxifier population were picked and whole-genome sequenced following the
601 same workflow. All of the sequences can be accessed at the NCBI Sequence Read Archive
602 (http://www.ncbi.nlm.nih.gov/sra) under Bioproject ID number PRJNA947372. The sequence
603 alignment was performed between ancestors and evolved clones.

604 **Formulation of the mathematical model and the simulation protocols**

605 The mathematical model was built to characterize the dynamics of a community composed of
606 two strains (a Degrader and a Detoxifier). The model is built on seven assumptions based on
607 our experimental system, in which the first three are the key assumptions that we emphasized
608 in the Result section.

609 (1) The consortium may grow in two environments that enable two different types of

610 interactions between the two strains. In the environment where the two strains engage in
611 facultatively mutualistic cooperation (environment (Mutual.)), the Degrader strain grows on an
612 initial substrate (S) and degrades S into a toxic intermediate (I) that is metabolized by the
613 Detoxifier strain for detoxification. In the other environment, the two strains can grow
614 independently (environment (Comp.)).
615 (2) the Autonomy may evolve from either population via horizontal gene transfer (HGT) in
616 both environments. After an HGT event, the biomass of the evolved autonomous genotype
617 follows a Poisson distribution with an expectation proportional to the biomass of both the
618 Degrader and Detoxifier[63,64].
619 (3) the evolved Autonomy population has a competitive edge (in terms of both the growth rate
620 and carrying capacity) against the two cooperative specialists in the environment (Mutual.) but
621 grows slower than them in the environment (Comp.).
622 (4) the models were built on a well-mixed system.
623 (5) the supply of naphthalene is sufficient in the environment (Mutual.), so the rate of S
624 consumption remains constant, and the specific growth rate of the Degrader remains constant.
625 (6) the intracellular accumulation of I is negligible, so the consumption rate of I follows the
626 first-order kinetics, and the specific growth rate of the Detoxifier is proportional to the
627 concentration of I.
628 (7) the degradation rate of S and the consuming rate of I are proportional to the biomass of the
629 relevant population.
630 These assumptions enable us to build minimal models to describe the growth dynamics of the
631 consortium in the two environments. The population dynamics of one growth cycle in the
632 environment (Mutual.) are given by

633 $$\frac{di}{d\tau} = a_1 \cdot x_1 - a_2 \cdot i \cdot (x_2 + x_3 + x_4) \quad [2]$$

634 $$\frac{dx_1}{d\tau} = \mu_{m,Degra} x_1 \left(1 - \frac{x_1 + x_2 + co \cdot (x_3 + x_4)}{\rho_m}\right) - m_1 - k_i \cdot i \cdot x_1 \quad [3]$$

$$\frac{dx_2}{d\tau} = a_2 \cdot i \cdot y \cdot x_2 \left(1 - \frac{x_1+x_2+co\cdot(x_3+x_4)}{\rho_d}\right) - m_2 - k_i \cdot i \cdot x_2 \quad [4]$$

$$\frac{dx_3}{d\tau} = m_1 + \sigma_m \mu_{m,Degra} \cdot x_3 \left(1 - \frac{x_1+x_2+co\cdot(x_3+x_4)}{\rho_m}\right) - k_i \cdot i \cdot x_3 \quad [5]$$

$$\frac{dx_4}{d\tau} = m_2 + \sigma_m \mu_{m,Degra} \cdot x_4 \left(1 - \frac{x_1+x_2+co\cdot(x_3+x_4)}{\rho_m}\right) - k_i \cdot i \cdot x_4 \quad [6]$$

The population dynamics of one growth cycle in the environment (Comp.) are given by

$$\frac{dx_1}{d\tau} = \mu_{c,Degra} x_1 \left(1 - \frac{x_1+x_2+x_3+x_4}{\rho_c}\right) - m_1 \quad [7]$$

$$\frac{dx_2}{d\tau} = \sigma_{c,Detox} \cdot \mu_{c,Degra} x_2 \left(1 - \frac{x_1+x_2+x_3+x_4}{\rho_c}\right) - m_2 \quad [8]$$

$$\frac{dx_3}{d\tau} = \sigma_{c,A} \cdot \mu_{c,Degra} x_3 \left(1 - \frac{x_1+x_2+x_3+x_4}{\rho_c}\right) + m_1 \quad [9]$$

$$\frac{dx_4}{d\tau} = \sigma_{c,A} \cdot \mu_{c,Degra} x_4 \left(1 - \frac{x_1+x_2+x_3+x_4}{\rho_c}\right) + m_2 \quad [10]$$

In the model, τ is the time. x_1 is the biomass of the Degrader while x_2 is that of the Detoxifier. x_3 and x_4 represent the biomass of the Autonomy that evolve from the Degrader and the Detoxifier, respectively. i represents the concentration of the intermediate in the environment (Mutual.). a_1 and a_2 are the rates of the two reactions (S to I and I to P). y is the biomass yield coefficient of the Detoxifier utilizing I. $\mu_{m,Degra}$ is the growth rate of the Degrader in the environment (Mutual.). σ_m represents the relative growth rate of Autonomy to that of the Degrader in the environment (Mutual.). Similarly, $\mu_{c,Degra}$ is the growth rate of the Degrader in the environment (Comp.). $\sigma_{c,Detox}$ and $\sigma_{c,A}$ represent the relative growth rate of the Detoxifier and Autonomy to that of the Degrader in the environment (Comp.). ρ_m and ρ_c represent the carrying capacity of all populations in the environment (Mutual.) and (Comp.), respectively. co evaluates the competitive edge of the Autonomy against the Degrader and Detoxifier. m_1 and m_2 are the biomass of the evolved Autonomy after an HGT event, which follows a poison distribution with an expectation of $\varepsilon \cdot x_1 x_2$, where ε evaluates the HGT rate.

656 To model the evolutionary dynamics of the mutualistic consortium, simulations were
657 performed by serially passaging a consortium initially composed of Degrader and Detoxifier
658 for 50 or 100 cycles with two conditions identical to our experiments: (1) the mutulism
659 condition, in which the simulations were performed continuously using the equations [2] - [6]
660 that characterize community dynamics in the environment (Mutual.); (2) the fluctuating
661 condition, in which the simulations were performed alternately using the two equation systems.
662 Since the evolved autonomous genotype can never dominate the community if only the
663 environment (Comp.) is given according to the third assumption, the modeling of the
664 competition condition was not performed. For each cycle, the consortium is allowed to grow
665 to the early stationary phase (when the total biomass reaches 99.9% of the carrying capacity),
666 mimicking the experiments. The consortium was then diluted to a novel cycle with a dilution
667 factor of d.
668 To mathematically predict the experimental results, parameter values matching our
669 experimental system[88] (Table S3: the default values) were applied to the model. To investigate
670 the key factors determining when fluctuating environments benefit the evolution of Autonomy
671 from mutualistic cooperation, 17501 parameter sets were generated by randomly picking the
672 values of the 14 main parameters from the given ranges (Table S3). The ranges were chosen
673 by incorporating at least ~10-fold higher or lower than the default value. For each parameter
674 set, simulations with the mutualism condition and the fluctuating condition were performed,
675 and 20 replicates were set for each condition to capture the randomness in the evolution. The
676 dynamics of different populations (i.e., x_1, x_2, x_3, and x_4) were recorded for further analysis.
677 To identify the key factors determining the evolution of Autonomy from mutualistic
678 cooperation, several Indices were defined for correlation analysis. First, BCI_M and BCI_C were
679 defined to evaluate the cell density and coexistence level in the environment (Mutual.) and
680 (Comp.), which are formulated as

681 $$BCI_M = B_{M,\ Degra} \cdot B_{M,\ Detox} \quad [11]$$

682 $$BCI_C = B_{C,\ Degra} \cdot B_{C,\ Detox} \quad [12]$$

683 Here, $B_{M,\ Degra}$ is the biomass of the Degrader (x_1) when the total biomass reaches 99.9% of
684 the carrying capacity in the environment (Mutual.) while $B_{M,\ Detox}$ is that of the Detoxifier (x_2).
685 $B_{C,\ Degra}$ and $B_{C,\ Detox}$ represent the same values in the environment (Comp.). Thus, the two *BCI*
686 values are proportional to the total biomass and community evenness (The closer the relative
687 abundances of the Degrader and Detoxifier, the higher evenness of the consortium, and the *BCI*
688 values are also higher). Relative Biomass-Coexistence Indice ($BCI_{C/M}$) was then defined to
689 characterize the relative cell density and coexistence levels in the environment (Comp.) than
690 that in the environment (Mutual.), calculated by

691 $$BCI_{C/M} = ln \frac{BCI_C}{BCI_M} \quad [13]$$

692 To evaluate the growth duration of the consortium in the two environments, T_C and T_M were
693 introduced. T_C indicates the duration of the growth of the consortium to a total biomass
694 reaching 99.9% of the carrying capacity in the environment (Comp.) while T_M indicates that
695 duration in the environment (Mutual.). Accordingly, the Relative Duration of growing in the
696 environment (Comp.) versus the environment (Mutual.) ($T_{C/M}$) is defined as

697 $$T_{C/M} = ln \frac{T_C}{T_M} \quad [14]$$

698 Finally, P_{fluc} and P_{mut} are used to quantify the probabilities of the evolution of Autonomy in the
699 fluctuating and mutualism conditions. P_{fluc} indicates the frequency of the simulations in which
700 the Autonomy dominates the community among 20 replicated simulations in the fluctuating
701 condition while P_{mut} is that in the mutualism condition. The Fluctuation-Benefiting Indice (FBI)
702 quantifies whether environmental fluctuation is beneficial for the evolution of Autonomy,
703 calculated by

704 $$FBI = P_{fluc} - P_{mut} \quad [15]$$

All the simulations, as well as the downstream analysis, were performed using custom Mathematica scripts. The source codes used for the model analysis are publicly available (Mendeley Data, doi: 10.17632/rbn7cwb4hn.1).

Quantification and statistical analyses

The statistical methods are described in figure legends. For the linear fit of the simulation data, the data were first normalized by the maximum and minimum values, and the analyses were performed using the LinearModelFit function in *Wolfram Mathematica* (version 12.0) with default settings. The values of adjusted R-squared can be found in all related figures. Student's T-test, Kolmogorov-Smirnov Test, and Pearson correlation analysis were calculated using the custom Mathematica scripts. To avoid the impact of the data size on significance analysis, the Student's T-tests and Kolmogorov-Smirnov Tests of the simulation datasets were carried out with 1000 values randomly selected from each group sample.

Replication and randomization

Replicate experiments have been performed for all key data shown in this study. Biological or technical replicate samples were randomized where appropriate. The numbers of replicates are listed in the related figure legends.

Acknowledgments

We thank the members of the Wu lab at Peking University and Microbial Systems Ecology group at ETH Zürich for the critical discussions of this work. We thank Mr. Chunhui Hao from Oxford University for his helpful suggestions on the term usage in this study. We thank Dr. T. Juelich (UCAS, Beijing) for linguistic assistance during the preparation of this manuscript. We would like to express our gratitude to the organizers of the EMBO Workshop (Molecular Mechanisms in Evolution and Ecology) for providing us with the opportunity to present this work in the picturesque city of Heidelberg in the autumn of 2022. We also thank the Young Scholars Forum (2022) organized by the journal *mLife* for allowing us to showcase this research.

We wish to extend our appreciation to the attendees of these conferences for their valuable feedback, which helped us a lot to improve our study. Miaoxiao Wang wishes to express his heartfelt gratitude to his wife, Yaxi Li, for her unwavering support and encouragement throughout this research project. This work was supported by National Key R&D Program of China (2018YFA0902100 and 2018YFA0902103), National Natural Science Foundation of China (91951204, 31761133006, 31770120, and 31770118), and Sino Swiss Science and Technology Cooperation (SSSTC) Program (IZLCZ0_206044).

Author Contributions

XC, MW, and YN conceived the study. XC and MW designed the evolution experiments. XC performed the experiments and analyzed the experimental data. MW constructed the ODE model, performed mathematical simulations, and analyzed the simulation data. MW drafted the manuscript with the help of XC. XC, YN, and XLW revised the manuscript. MW, YN, and XLW raised the funding for the project.

1 Rueffler, C., Hermisson, J. & Wagner, G. P. Evolution of functional specialization and division of labor. *Proc Natl Acad Sci U S A* **109**, E326-335, doi:10.1073/pnas.1110521109 (2012).
2 Goldsby, H. J., Dornhaus, A., Kerr, B. & Ofria, C. Task-switching costs promote the evolution of division of labor and shifts in individuality. *Proc Natl Acad Sci U S A* **109**, 13686-13691, doi:10.1073/pnas.1202233109 (2012).
3 Karanth, K. U. & Sunquist, M. E. Behavioural correlates of predation by tiger (Panthera tigris), leopard (Panthera pardus) and dhole (Cuon alpinus) in Nagarahole, India. *Journal of Zoology* **250**, 255-265 (2000).
4 Eaton, R. L. Hunting behavior of the cheetah. *The Journal of Wildlife Management*, 56-67 (1970).
5 Collopy, M. W. Foraging behavior and success of Golden Eagles. *The Auk* **100**, 747-749 (1983).
6 Stander, P. E. Cooperative hunting in lions: the role of the individual. *Behavioral ecology and sociobiology* **29**, 445-454 (1992).
7 Watts, H. E. & Holekamp, K. E. Hyena societies. *Curr Biol* **17**, R657-660, doi:10.1016/j.cub.2007.06.002 (2007).
8 Pitman, R. L. & Durban, J. W. Cooperative hunting behavior, prey selectivity and prey handling by pack ice killer whales (Orcinus orca), type B, in Antarctic Peninsula waters. *Marine Mammal Science* **28**, 16-36 (2012).
9 Bednarz, J. C. Cooperative Hunting Harris' Hawks (Parabuteo unicinctus). *Science* **239**, 1525-1527, doi:10.1126/science.239.4847.1525 (1988).
10 Straka, L. L., Meinhardt, K. A., Bollmann, A., Stahl, D. A. & Winkler, M. K. H. Affinity informs environmental cooperation between ammonia-oxidizing archaea (AOA) and anaerobic ammonia-oxidizing (Anammox) bacteria. *Isme J* **13**, 1997-2004, doi:10.1038/s41396-019-0408-x (2019).
11 Kuypers, M. M. M. A division of labour combined. *Nature* **528**, 487–488 (2015).
12 van Kessel, M. A. *et al.* Complete nitrification by a single microorganism. *Nature* **528**, 555-559, doi:10.1038/nature16459 (2015).
13 Daims, H. *et al.* Complete nitrification by Nitrospira bacteria. *Nature* **528**, 504-509, doi:10.1038/nature16461 (2015).
14 Antje Boetius, K. R., Carsten J. Schubert, Dirk Rickert, Friedrich Widdel, Armin Gieseke, Rudolf Amann, Bo Barker Jørgensen, Ursula Witte & Olaf Pfannkuche A marine microbial consortium apparently mediating anaerobic oxidation of methane. *Nature* **407**, 623–626 (2000).
15 Zhou, Z. *et al.* Non-syntrophic methanogenic hydrocarbon degradation by an archaeal species. *Nature* **601**, 257-262, doi:10.1038/s41586-021-04235-2 (2022).
16 Sachs, J. L. & Simms, E. L. Pathways to mutualism breakdown. *Trends Ecol Evol* **21**, 585-592, doi:10.1016/j.tree.2006.06.018 (2006).
17 Miaoxiao, W., Xiaonan, L., Yong, N. & Xiao-Lei, W. Selfishness driving reductive evolution shapes interdependent patterns in spatially structured microbial communities. *The ISME Journal* **15**, 1387--1401, doi:10.1038/s41396-020-00858-x (2020).
18 Costa, E., Pérez, J. & Kreft, J.-U. Why is metabolic labour divided in nitrification? *Trends in microbiology* **14**, 213-219 (2006).
19 Ryan, T. *et al.* Metabolic division of labor in microbial systems. *Proceedings of the National Academy of Sciences* **115**, 2526--2531, doi:10.1073/pnas.1716888115 (2018).
20 Cooper, G. A., Frost, H., Liu, M. & West, S. A. The evolution of division of labour in structured and unstructured groups. *Elife* **10**, doi:10.7554/eLife.71968 (2021).
21 Goyal, A. Horizontal gene transfer drives the evolution of dependencies in bacteria. *Iscience* **25**, 104312, doi:10.1016/j.isci.2022.104312 (2022).
22 Mas, A., Jamshidi, S., Lagadeuc, Y., Eveillard, D. & Vandenkoornhuyse, P. Beyond the Black Queen Hypothesis. *Isme J* **10**, 2085-2091, doi:10.1038/ismej.2016.22 (2016).
23 Morris, J. J., Lenski, R. E. & Zinser, E. R. The Black Queen Hypothesis: evolution of dependencies through adaptive gene loss. *Mbio* **3**, doi:10.1128/mBio.00036-12 (2012).
24 Morris, J. J. Black Queen evolution: the role of leakiness in structuring microbial communities. *Trends Genet* **31**, 475-482, doi:10.1016/j.tig.2015.05.004 (2015).
25 Billet, L., Devers, M., Rouard, N., Martin-Laurent, F. & Spor, A. Labour sharing promotes coexistence in atrazine degrading bacterial communities. *Scientific Reports* **9**, doi:ARTN 18363 10.1038/s41598-019-54978-2 (2019).
26 Morris, J. J., Papoulis, S. E. & Lenski, R. E. Coexistence of evolving bacteria stabilized by a shared Black Queen function. *Evolution* **68**, 2960-2971, doi:10.1111/evo.12485 (2014).
27 Cordero, O. X., Ventouras, L. A., DeLong, E. F. & Polz, M. F. Public good dynamics drive evolution of iron acquisition strategies in natural bacterioplankton populations. *Proc Natl Acad Sci U S A* **109**, 20059-

20064, doi:10.1073/pnas.1213344109 (2012).
28 Souza, L. S., Irie, Y. & Eda, S. Black Queen Hypothesis, partial privatization, and quorum sensing evolution. *Plos One* **17**, doi:10.1371/journal.pone.0278449 (2022).
29 Kim, W., Levy, S. B. & Foster, K. R. Rapid radiation in bacteria leads to a division of labour. *Nat Commun* **7**, doi:ARTN 10508
10.1038/ncomms10508 (2016).
30 Campbell, K. *et al.* Self-establishing communities enable cooperative metabolite exchange in a eukaryote. *Elife* **4**, doi:ARTN e09943
10.7554/eLife.09943 (2015).
31 Pauli, B., Ona, L., Hermann, M. & Kost, C. Obligate mutualistic cooperation limits evolvability. *Nat Commun* **13**, doi:ARTN 337
10.1038/s41467-021-27630-9 (2022).
32 Dragoš, A. *et al.* Collapse of genetic division of labour and evolution of autonomy in pellicle biofilms. *Nature Microbiology*, doi:10.1038/s41564-018-0263-y (2018).
33 Arnold, B. J., Huang, I. T. & Hanage, W. P. Horizontal gene transfer and adaptive evolution in bacteria. *Nat Rev Microbiol* **20**, 206-218, doi:10.1038/s41579-021-00650-4 (2022).
34 Wang, T. *et al.* Horizontal gene transfer enables programmable gene stability in synthetic microbiota. *Nat Chem Biol* **18**, 1245-1252, doi:10.1038/s41589-022-01114-3 (2022).
35 Hall, C. & Dietrich, F. S. The reacquisition of biotin prototrophy in Saccharomyces cerevisiae involved horizontal gene transfer, gene duplication and gene clustering. *Genetics* **177**, 2293-2307, doi:10.1534/genetics.107.074963 (2007).
36 Hall, C., Brachat, S. & Dietrich, F. S. Contribution of horizontal gene transfer to the evolution of Saccharomyces cerevisiae. *Eukaryot Cell* **4**, 1102-1115, doi:10.1128/EC.4.6.1102-1115.2005 (2005).
37 Chu, H. Y., Sprouffske, K. & Wagner, A. Assessing the benefits of horizontal gene transfer by laboratory evolution and genome sequencing. *Bmc Evol Biol* **18**, 54, doi:10.1186/s12862-018-1164-7 (2018).
38 Nguyen, J., Lara-Gutierrez, J. & Stocker, R. Environmental fluctuations and their effects on microbial communities, populations and individuals. *Fems Microbiology Reviews* **45**, doi:ARTN fuaa068
10.1093/femsre/fuaa068 (2021).
39 Rodriguez-Verdugo, A. & Ackermann, M. Rapid evolution destabilizes species interactions in a fluctuating environment. *ISME J*, doi:10.1038/s41396-020-00787-9 (2020).
40 Cvijovic, I., Good, B. H., Jerison, E. R. & Desai, M. M. Fate of a mutation in a fluctuating environment. *P Natl Acad Sci USA* **112**, E5021-E5028, doi:10.1073/pnas.1505406112 (2015).
41 Chesson, P. Mechanisms of maintenance of species diversity. *Annu Rev Ecol Syst* **31**, 343-366, doi:DOI 10.1146/annurev.ecolsys.31.1.343 (2000).
42 Chesson, P. L. Environmental variation and the coexistence of species. *Community ecology* **240**, 54 (1986).
43 Jiang, L. & Morin, P. J. Temperature fluctuation facilitates coexistence of competing species in experimental microbial communities. *Journal of animal ecology*, 660-668 (2007).
44 Wang, M. *et al.* Even allocation of benefits stabilizes microbial community engaged in metabolic division of labor. *Cell Reports* **40**, 111410, doi:10.1016/j.celrep.2022.111410 (2022).
45 Mariana, P. L. *et al.* Physiological role of NahW , the additional salicylate hydroxylase found in$\less$i$\greater$Pseudomonas stutzeri$\less$/i$\greater$ AN 10. *FEMS Microbiology Letters* **300**, 265--272, doi:10.1111/j.1574-6968.2009.01787.x (2009).
46 Miaoxiao, W., Xiaoli, C., Yue-Qin, T., Yong, N. & Xiao-Lei, W. Substrate availability and toxicity shape the structure of microbial communities engaged in metabolic division of labor. *mLife* **1**, 131--145, doi:10.1002/mlf2.12025 (2022).
47 Peng, X. F. *et al.* Genomic and functional analyses of fungal and bacterial consortia that enable lignocellulose breakdown in goat gut microbiomes. *Nat Microbiol* **6**, 499-+, doi:10.1038/s41564-020-00861-0 (2021).
48 Dombrowski, N. *et al.* Reconstructing metabolic pathways of hydrocarbon-degrading bacteria from the Deepwater Horizon oil spill. *Nat Microbiol* **1**, doi:Artn 16057
10.1038/Nmicrobiol.2016.57 (2016).
49 Schink, B. & Pfennig, N. Fermentation of Trihydroxybenzenes by Pelobacter-Acidigallici Gen-Nov Sp-Nov a New Strictly Anaerobic, Non-Sporeforming Bacterium. *Arch Microbiol* **133**, 195-201, doi:Doi 10.1007/Bf00415000 (1982).
50 Wang, C. Y., Huang, Y., Zhang, Z. T., Hao, H. & Wang, H. Absence of the nahG-like gene caused the syntrophic interaction between Marinobacter and other microbes in PAH-degrading process. *J Hazard*

858 *Mater* **384**, doi:ARTN 121387
859 10.1016/j.jhazmat.2019.121387 (2020).
860 51 Jia, X. Q., He, Y., Jiang, D. W., Liu, C. & Lu, W. Y. Construction and analysis of an engineered Escherichia
861 coli-Pseudomonas aeruginosa co-culture consortium for phenanthrene bioremoval. *Biochem Eng J* **148**,
862 214-223, doi:10.1016/j.bej.2019.05.010 (2019).
863 52 Li, C. M., Wu, H. Z., Wang, Y. X., Zhu, S. & Wei, C. H. Enhancement of phenol biodegradation: Metabolic
864 division of labor in co-culture of Stenotrophomonas sp. N5 and Advenella sp. B9. *J Hazard Mater* **400**,
865 123214, doi:10.1016/j.jhazmat.2020.123214 (2020).
866 53 Gilbert, E. S., Walker, A. W. & Keasling, J. D. A constructed microbial consortium for biodegradation of
867 the organophosphorus insecticide parathion. *Appl Microbiol Biot* **61**, 77-81, doi:10.1007/s00253-002-
868 1203-5 (2003).
869 54 Kato, S., Haruta, S., Cui, Z. J., Ishii, M. & Igarashi, Y. Stable coexistence of five bacterial strains as a
870 cellulose-degrading community. *Appl Environ Microb* **71**, 7099-7106, doi:10.1128/Aem.71.11.7099-
871 7106.2005 (2005).
872 55 Robin, T. & Dani, O. Cooperation in carbon source degradation shapes spatial self-organization of
873 microbial consortia on hydrated surfaces. *Scientific Reports* **7**, doi:10.1038/srep43726 (2017).
874 56 Dragos, A. *et al.* Collapse of genetic division of labour and evolution of autonomy in pellicle biofilms.
875 *Nat Microbiol* **3**, 1451-1460, doi:10.1038/s41564-018-0263-y (2018).
876 57 Phale, P. S., Shah, B. A. & Malhotra, H. Variability in Assembly of Degradation Operons for Naphthalene
877 and its derivative, Carbaryl, Suggests Mobilization through Horizontal Gene Transfer. *Genes (Basel)* **10**,
878 doi:10.3390/genes10080569 (2019).
879 58 Zhang, X. M. *et al.* Stress-Induced, Highly Efficient, Donor Cell-Dependent Cell-to-Cell Natural
880 Transformation in Bacillus subtilis. *Journal of Bacteriology* **200**, doi:ARTN e00267-18
881 10.1128/JB.00267-18 (2018).
882 59 Arnold, B. J., Huang, I. T. & Hanage, W. P. Horizontal gene transfer and adaptive evolution in bacteria.
883 *Nat Rev Microbiol*, doi:10.1038/s41579-021-00650-4 (2021).
884 60 Groussin, M. *et al.* Elevated rates of horizontal gene transfer in the industrialized human microbiome.
885 *Cell* **184**, 2053-+, doi:10.1016/j.cell.2021.02.052 (2021).
886 61 van Elsas, J. D. & Bailey, M. J. The ecology of transfer of mobile genetic elements. *Fems Microbiol Ecol*
887 **42**, 187-197, doi:Pii S0168-6496(02)00373-2
888 Doi 10.1016/S0168-6496(02)00373-2 (2002).
889 62 Madsen, J. S., Burmolle, M., Hansen, L. H. & Sorensen, S. J. The interconnection between biofilm
890 formation and horizontal gene transfer. *Fems Immunol Med Mic* **65**, 183-195, doi:10.1111/j.1574-
891 695X.2012.00960.x (2012).
892 63 Mao, J. & Lu, T. Population-Dynamic Modeling of Bacterial Horizontal Gene Transfer by Natural
893 Transformation. *Biophys J* **110**, 258-268, doi:10.1016/j.bpj.2015.11.033 (2016).
894 64 Novozhilov, A. S., Karev, G. P. & Koonin, E. V. Mathematical modeling of evolution of horizontally
895 transferred genes. *Molecular biology and evolution* **22**, 1721-1732 (2005).
896 65 Smith, A. *The wealth of nations [1776]*. Vol. 11937 (na, 1937).
897 66 Cooper, G. A. & West, S. A. Division of labour and the evolution of extreme specialization. *Nature Ecology*
898 *& Evolution* **2**, 1161-+, doi:10.1038/s41559-018-0564-9 (2018).
899 67 Liu, M., West, S. A. & Cooper, G. A. Relatedness and the evolution of mechanisms to divide labor in
900 microorganisms. *Ecol Evol* **11**, 14475-14489, doi:10.1002/ece3.8067 (2021).
901 68 Rueffler, C., Hermisson, J. & Wagner, G. P. Evolution of functional specialization and division of labor. *P*
902 *Natl Acad Sci USA* **109**, E326-E335, doi:10.1073/pnas.1110521109 (2012).
903 69 Chomicki, G., Kiers, E. T. & Renner, S. S. The Evolution of Mutualistic Dependence. *Annu Rev Ecol Evol S*
904 **51**, 409-432, doi:10.1146/annurev-ecolsys-110218-024629 (2020).
905 70 Preussger, D., Giri, S., Muhsal, L. K., Ona, L. & Kost, C. Reciprocal Fitness Feedbacks Promote the
906 Evolution of Mutualistic Cooperation. *Curr Biol* **30**, 3580-3590 e3587, doi:10.1016/j.cub.2020.06.100
907 (2020).
908 71 Tognon, M. *et al.* Co-evolution with Staphylococcus aureus leads to lipopolysaccharide alterations in
909 Pseudomonas aeruginosa. *Isme J* **11**, 2233-2243, doi:10.1038/ismej.2017.83 (2017).
910 72 Hu, H. *et al.* Guided by the principles of microbiome engineering: Accomplishments and perspectives
911 for environmental use. *mLife* **1**, 382-398, doi:https://doi.org/10.1002/mlf2.12043 (2022).
912 73 Xie, L. & Shou, W. Y. Steering ecological-evolutionary dynamics to improve artificial selection of
913 microbial communities. *Nat Commun* **12**, doi:ARTN 6799
914 10.1038/s41467-021-26647-4 (2021).

74 Chang, C. Y. *et al.* Engineering complex communities by directed evolution. *Nature Ecology & Evolution* **5**, 1011-+, doi:10.1038/s41559-021-01457-5 (2021).
75 Rodriguez-Verdugo, A. & Ackermann, M. Rapid evolution destabilizes species interactions in a fluctuating environment. *Isme J* **15**, 450-460, doi:10.1038/s41396-020-00787-9 (2021).
76 Chen, X. *et al.* High immigration rates critical for establishing emigration-driven diversity in microbial communities. *bioRxiv*, 2023.2002. 2024.529875 (2023).
77 Abreu, C. I., Friedman, J., Woltz, V. L. A. & Gore, J. Mortality causes universal changes in microbial community composition. *Nat Commun* **10**, doi:ARTN 2120 10.1038/s41467-019-09925-0 (2019).
78 Cira, N. J., Pearce, M. T. & Quake, S. R. Neutral and selective dynamics in a synthetic microbial community. *P Natl Acad Sci USA* **115**, E9842-E9848, doi:10.1073/pnas.1808118115 (2018).
79 Barber, J. N. *et al.* The evolution of coexistence from competition in experimental co-cultures of Escherichia coli and Saccharomyces cerevisiae. *Isme J* **15**, 746-761, doi:10.1038/s41396-020-00810-z (2021).
80 Choi, K. H. & Schweizer, H. P. Mini-Tn7 insertion in bacteria with single attTn7 sites: example Pseudomonas aeruginosa. *Nature Protocols* **1**, 153-161, doi:10.1038/nprot.2006.24 (2006).
81 Choi, K. H. & Schweizer, H. P. mini-Tn7 insertion in bacteria with single attTn7 sites: example Pseudomonas aeruginosa. *Nat Protoc* **1**, 153-161, doi:10.1038/nprot.2006.24 (2006).
82 Bosshard, L. *et al.* Accumulation of Deleterious Mutations During Bacterial Range Expansions. *Genetics* **207**, 669-684, doi:10.1534/genetics.117.300144 (2017).
83 Schafer, A. *et al.* Small mobilizable multi-purpose cloning vectors derived from the Escherichia coli plasmids pK18 and pK19: selection of defined deletions in the chromosome of Corynebacterium glutamicum. *Gene* **145**, 69-73, doi:10.1016/0378-1119(94)90324-7 (1994).
84 Gao, C. *et al.* NAD-Independent L-Lactate Dehydrogenase Required for L-Lactate Utilization in Pseudomonas stutzeri A1501. *J Bacteriol* **197**, 2239-2247, doi:10.1128/JB.00017-15 (2015).
85 Li, H. *et al.* Integrated electromicrobial conversion of CO_2 to higher alcohols. *Science* **335**, 1596, doi:10.1126/science.1217643 (2012).
86 Liang, J.-L. *et al.* Regulation of alkane degradation pathway by a TetR family repressor via an autoregulation positive feedback mechanism in a Gram-positiveDietziabacterium. *Molecular Microbiology* **99**, 338-359, doi:10.1111/mmi.13232 (2016).
87 Marshall, D. J. *et al.* Long-term experimental evolution decouples size and production costs in Escherichia coli. *Proc Natl Acad Sci U S A* **119**, e2200713119, doi:10.1073/pnas.2200713119 (2022).
88 Wang, M. X. *et al.* Even allocation of benefits stabilizes microbial community engaged in metabolic division of labor. *Cell Reports* **40**, doi:ARTN 111410 10.1016/j.celrep.2022.111410 (2022).

952 **Figures**

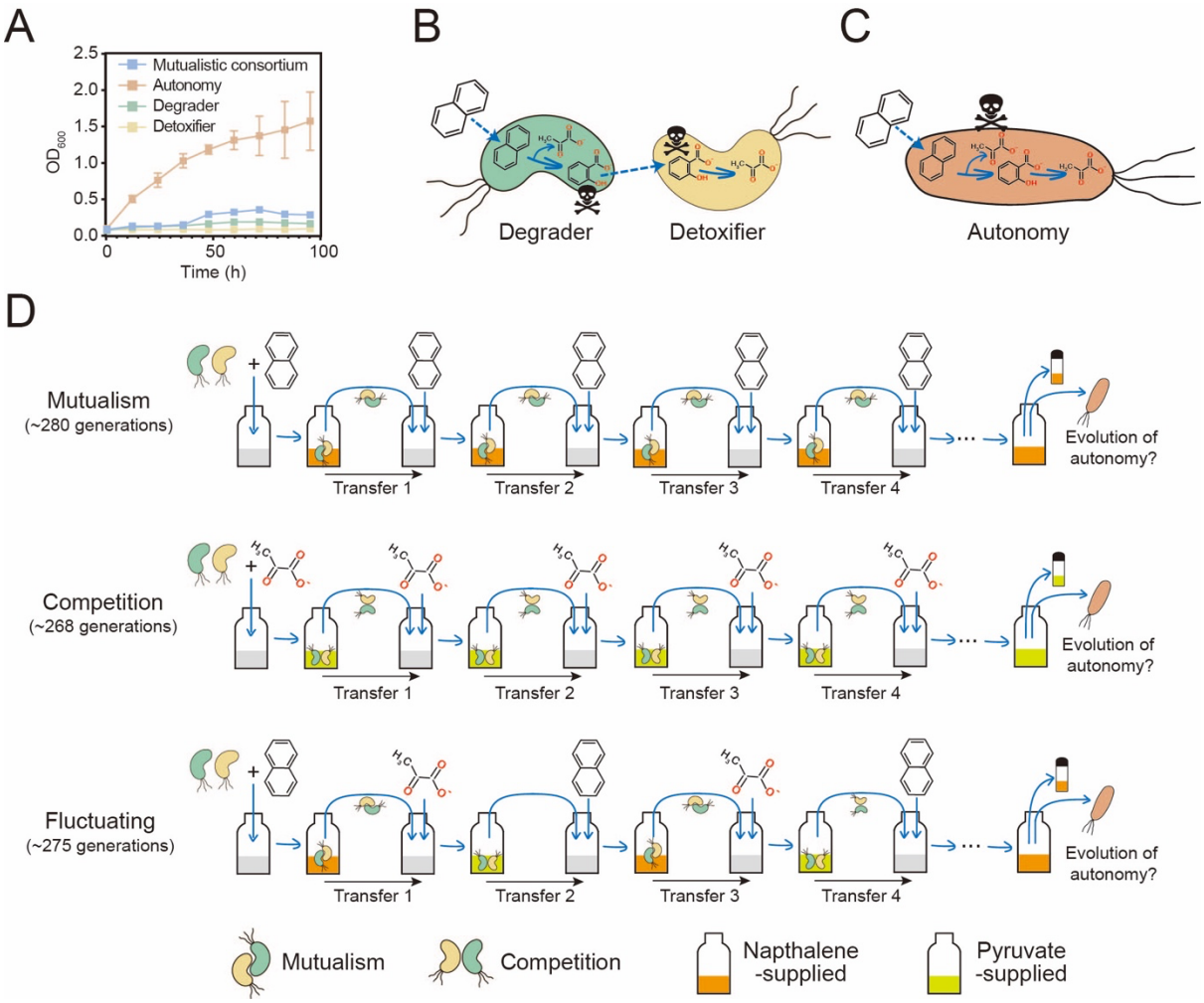

953

954 **Figure 1** The design of the experiments. (A) The growth curve of the synthetic consortium and
955 the Autonomy when naphthalene was supplied as the sole carbon source. (B) Schematic
956 diagram of our synthetic consortium performing mutualistic cooperation. The first strain,
957 termed Degrader, degrades naphthalene into an intermediate metabolite, salicylate, while the
958 second strain, termed Detoxifier, further metabolizes salicylate into pyruvate. (C) Schematic
959 diagram of our Autonomy strain that is capable of degrading naphthalene completely. (D)
960 Schematic diagram of the design of our evolution experiments. All the experiments started by
961 equally inoculating the Degrader and Detoxifier strains to the minimum medium. In the
962 condition of mutualism, naphthalene was supplied in every cycle, so the two strains in the
963 consortium engaged in mutualistic cooperation throughout the evolution. In the condition of

964 competition, pyruvate was supplied in every cycle so both strains grow competitively. In the
965 condition of fluctuating, naphthalene or pyruvate was alternately supplied in the passaging
966 cycles, so the two strains alternately engaged in mutualism or competition growth in different
967 cycles. The evolution underwent ~270 generations in each condition and we aim to address
968 whether an autonomous genotype can evolve from the mutualistic consortium.
969

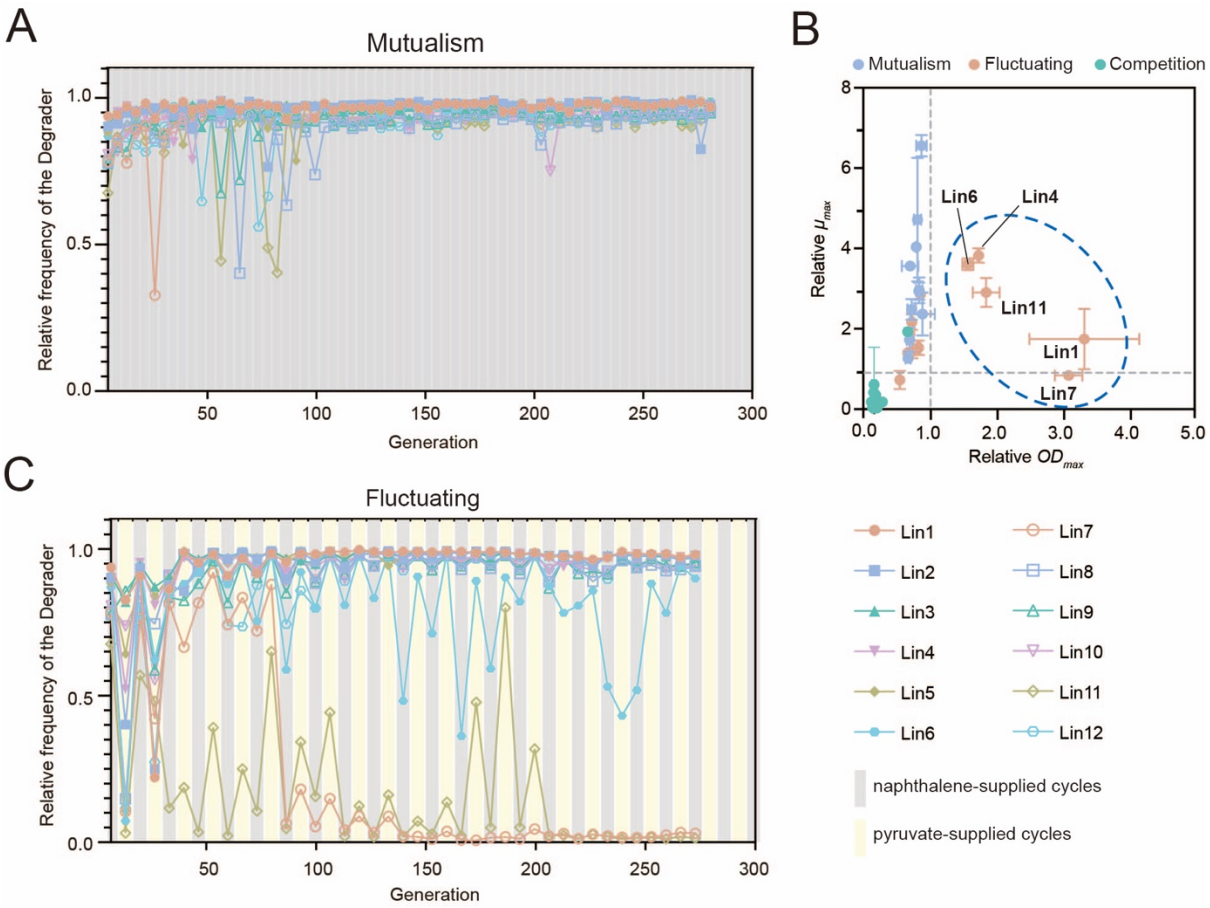

Figure 2 The dynamics of the mutualistic consortium in the evolution experiments under different conditions. (A, C) The dynamics of the community composition (denoted by the relative frequency of the Degrader strain) across all the evolutionary lineages in the mutualism (A) and the fluctuating condition (C). 12 independent replicates (i.e., lineages) were performed for each condition, which are distinguished by the curve legends shown on the right of (C). (B) Comparison of the growth kinetics between the evolved consortia and ancestral consortia. To determine their relative levels, we estimated the maximum cell density (OD_{max}) and the maximum growth rate (μ_{max}) of the evolved consortia in each condition and those of the ancestral consortia (n = 3). Dashed lines indicate levels of the ancestral consortia. The five lineages that have evolved under fluctuating conditions and exhibited higher growth kinetics to the ancestral consortia are circled and labeled.

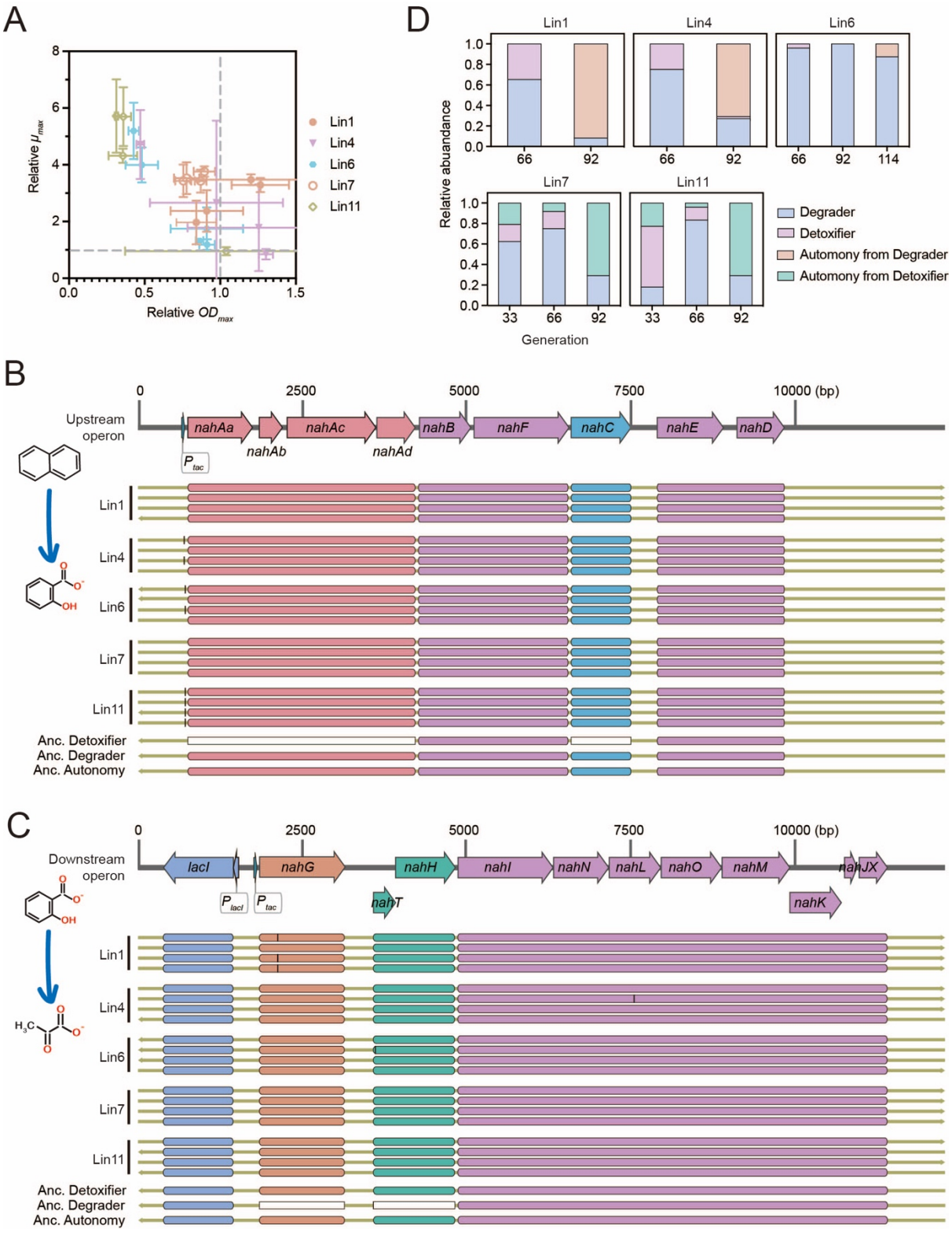

Figure 3 Autonomous populations evolved from our mutualistic consortium under fluctuating conditions. We focus on the five lineages (lineage 1, lineage 4, lineage 6, lineage 7, and lineage 11) that show approximate growth kinetics to the ancestral Autonomy strain after the evolution (See Figure 2). Four clonal isolates were picked from each evolved lineage. (A) Comparison

988 of the growth kinetics between the evolved isolates and ancestral Autonomy. To determine their
989 relative levels, we estimated the maximum cell density (OD_{max}) and the maximum growth rate
990 (μ_{max}) of the evolved isolates and those of the ancestral Autonomy strain (n = 3). Dashed lines
991 indicate levels of the ancestral Autonomy strain. (B-C) Comparative sequence analysis of two
992 naphthalene operons in ancestral and evolved populations. The first operon (B) contains the
993 genes responsible for the degradation of naphthalene to salicylate, while the second operon (C)
994 encodes the further conversion of the salicylate to pyruvate. The ancestral Detoxifier strain
995 lacks two key genes, *nahA* (Pink) and *nahC* (Blue), in the first operon, while the ancestral
996 Degrader strain lacks *nahG* (Orange) and *nahTH* (Green) in the second operon. These
997 mismatches are shown by the white boxes. Through the draft genomic sequencing, we found
998 all the evolved isolates regained these key genes. These regained genes locate exactly at the
999 same genomic locus as that of our ancestral Autonomy strain. The gene sequences are exactly
1000 the same except for several single-base mismatches (denoted by the black line). The directions
1001 of the arrows indicate the direction of the sequenced contigs. (D) Tracing the emergence of
1002 Autonomy during evolution. Through the isolation of 24 single clones and PCR genotyping
1003 (See Methods), we measured the relative abundances of Degrader, Detoxifier, and the evolved
1004 Autonomy at two or three different generations in the five lineages in which the Autonomy
1005 evolved under fluctuating conditions.
1006

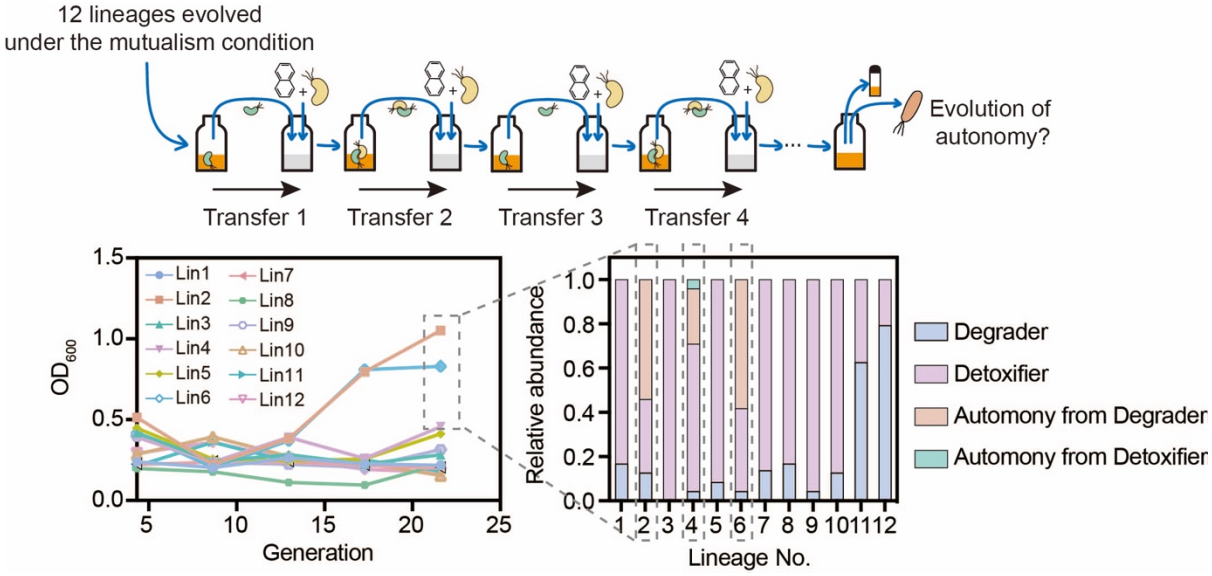

Figure 4 Supplementing the Detoxifier to the Degrader-dominated consortia favors the evolution of Autonomy. After our initial evolution experiments, Autonomy did not evolve in all twelve lineages under the mutualism condition. We then started a new evolution experiment of the ancestral consortium by reintroducing the Detoxifier when transferring the cultures to fresh media. The Detoxifier was reintroduced to the twelve lineages pre-evolved under the mutualism condition. After 22 generations, reintroducing the Detoxifier enabled the evolution of Autonomy in three out of twelve lineages. Notably, the analysis shows that the Autonomy genotype only evolved from the Degrader strain (i.e., the Degrader strain is the recipient of the horizontal gene transfer) under the fluctuating condition while the Autonomy genotype evolved from either Degrader or Detoxifier.

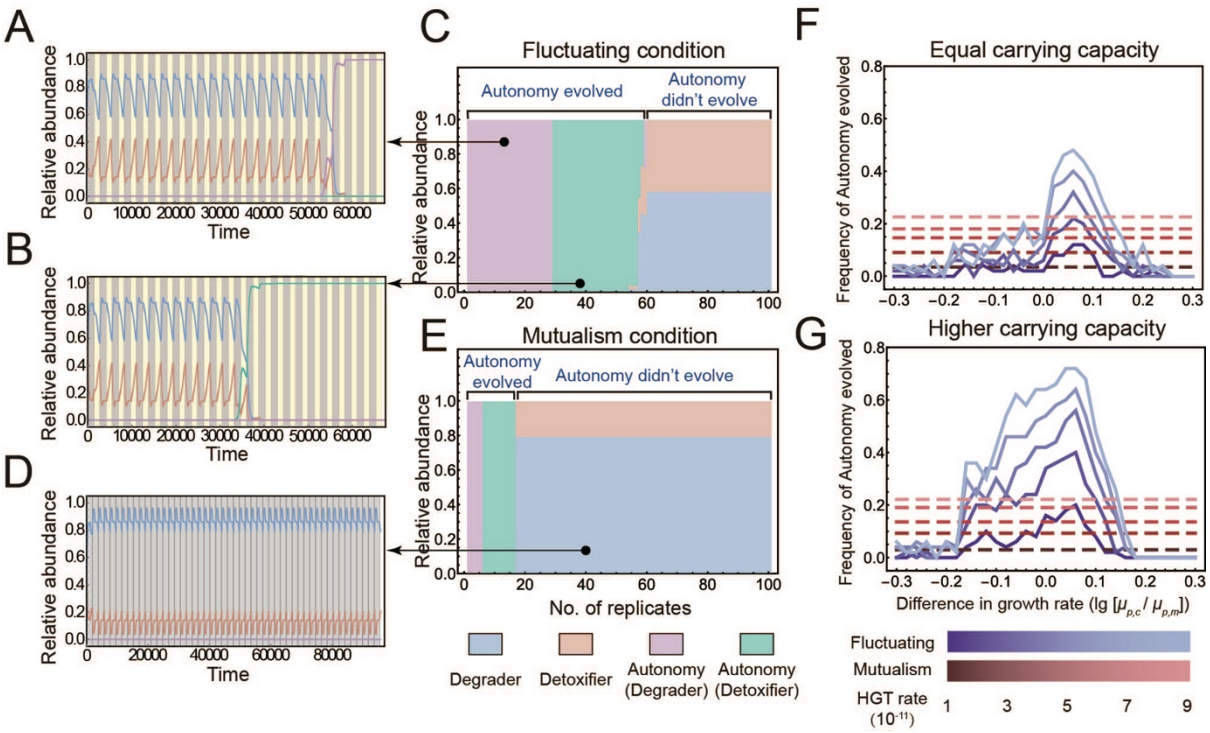

Figure 5 Representative simulations using our mathematical model capture the basic findings of our experiments. The simulations were initialized with the parameters measured from our experiment systems (Table S3: default values). Simulations under fluctuating and mutualism conditions were performed. (A-B) the relative abundance of different genotypes over the two representative simulations under the fluctuating condition, in which autonomy evolved from Degrader (A) or Detoxifier (B). (C) The summary of the evolutionary outcomes of 100 independent replicates was conducted for the fluctuating condition. (D) the relative abundance of different genotypes over a representative simulation under the mutualism condition. (E) The summary of the evolutionary outcomes of 100 independent replicates was conducted for the mutualism condition. (F-G) The correlation between the relative growth rate of the Detoxifier to that of the Degrader in the environment (comp.) and the frequency of Autonomy evolution was analyzed under two scenarios: (F) when the maximum carrying capacities of the two environments were the same; (G) the carrying capacity of the environment (Comp.) was set to be twice that of the environment (Mutual.). Unless specified otherwise, all these simulations were parameterized by the default values shown in Table S3.

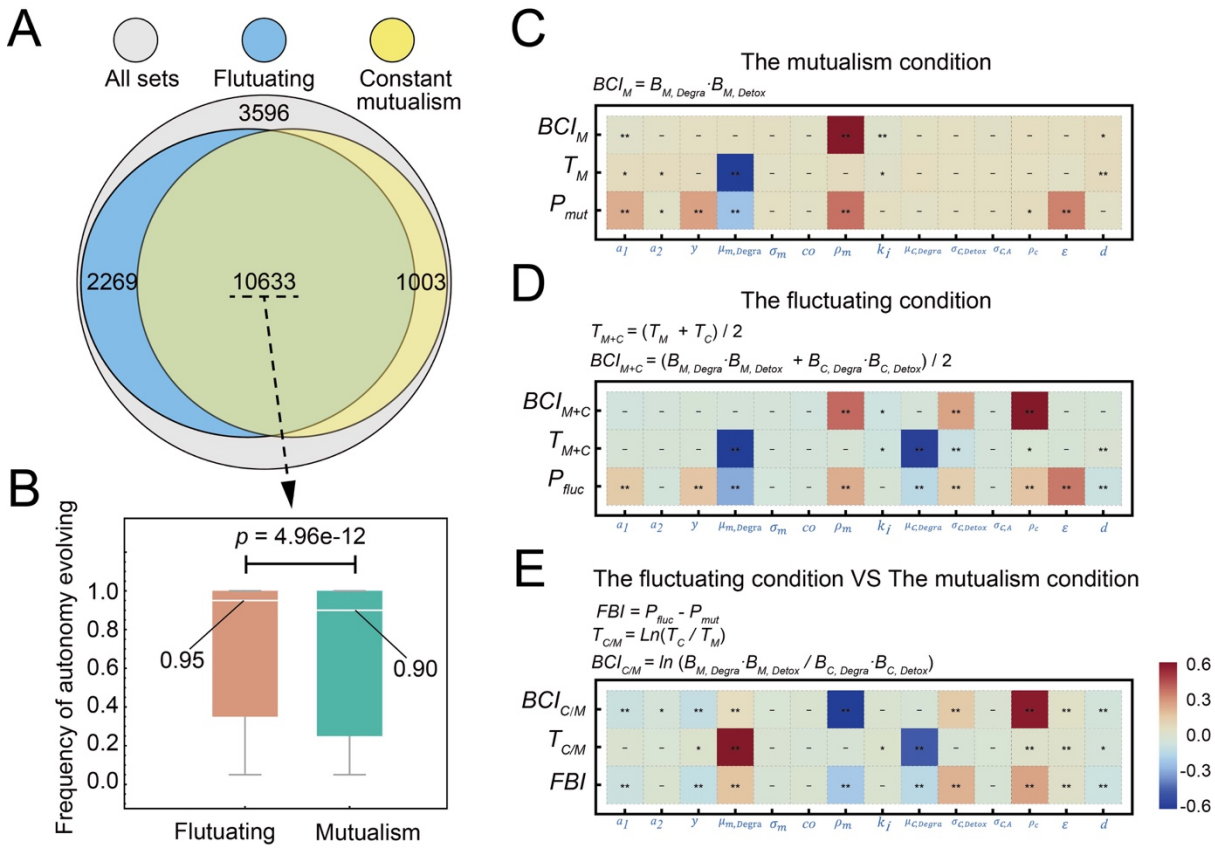

Figure 6 Generalizing our experimental findings using a mathematical model. We performed simulations using 17501 parameter sets that are generated based on random sampling from given value ranges (Table S3). For a given set, we modeled both the mutualism condition and the fluctuating condition with 20 replicates for each and calculated the frequency of the Autonomy evolution in both conditions (defined as P_{mut} and P_{fluc}). (A) a Venn diagram summarizes the evolutionary outcomes of all the simulations, indicating whether Autonomy evolved in both conditions (green), in either one of the conditions (blue and yellow), or in neither condition (Gray). (B) Comparison of the P_{mut} and P_{fluc} of the simulations where the autonomous genotype evolved in both fluctuating and mutualism conditions (the green section in (A)). The median values were indicated and pairwise Student's T-tests were performed to examine their significant difference. (C-E) Key factors determining the probability of the evolution of Autonomy under the mutualism condition (C) and the fluctuating condition (D), and whether fluctuating condition benefits the evolution of Autonomy (E). We performed the

Pearson correlation analysis between the parameter values and the frequency of the Autonomy evolution (P_{mut}, P_{fluc}, and FBI), the cell density and coexistence level in the two environments (BCI_M, BCI_C, and $BCI_{C/M}$), as well as the duration of growth in the two environments (T_M, T_C, and $T_{C/M}$). The Pearson correlation coefficients are shown by the color density, and the statistical significance of the analysis is shown ("*": $p < 0.01$; "**": $p < 0.0001$). Our results also show a positive correlation between P_{mut} and the BCI_M value ($R^2 = 0.28$; $p < 0.001$) in the mutualism condition, and a positive correlation with the average values of both BCI_M and BCI_C in the fluctuating condition ($R^2 = 0.39$; $p < 0.001$), suggesting that higher cell density and coexistence level benefit the evolution.